at 3700 MHz. At $\omega t = 0^\circ$, the predominant magnetic current is above the wide tuning stub and is oriented in a direction $\phi = 0^\circ$ relative to the $+x$ axis. At a later time instant with a 90° phase lagging ($\omega t = 90^\circ$), the principal magnetic current is along the open slot, whose direction is 90° relative to the $+x$ axis. At $\omega t = 180^\circ$ (270°), the magnetic current distribution is just opposite to that at $\omega t = 0^\circ$ (90°). The magnetic current distribution varying as a function of time in such a fashion can depict the behavior of predominantly right-and left-and CP radiations in the $z > 0$ and $z < 0$ half spaces, respectively.

Fig. 11 shows the measured and simulated far-field radiation patterns of Antenna 4 in the xz and yz planes at the center frequency of 3700 MHz. The far-field radiation patterns have lower AR values around the broadside directions (i.e., $\pm z$ directions). They are mainly RHCP for $z > 0$ and LHCP for $z < 0$. From Fig. 11, it is seen that measured and simulated results are with reasonable agreement. In 3-dB AR band (3.2–4.2 GHz), the measured and simulated results of peak antenna gain of Antenna 4 are shown in Fig. 12. It is found that the antenna gain has a maximum value of 5.3 dBic with a variation of less than 1 dBic. Also, the simulated efficiency is shown in Fig. 12. It is seen that the antenna efficiency is larger than 90% in the 3-dB AR band. Note that the measured gain is slightly higher than the simulated one. This is because of the influence from the cable of measurement system. In general, they are very close for each other.

IV. Conclusion

The novel broadband CPW-fed CP slot antenna has been demonstrated. The open slot can provide the perturbation into the wide slot antenna for the CP operation. Moreover, the use of wide tuning stub can improve the impedance and 3-dB AR bandwidths. Based on the parametric study, many prototypes have been successfully implemented. In addition to the simple uniplanar configuration, experimental results show that the proposed antenna has the impedance bandwidth of 111% for applications to 2–6 GHz WiMAX and the 3-dB AR bandwidth of 27% for applications to 3.3–3.8 GHz WiMAX. Under the use of inexpensive FR4 microwave substrate, the proposed antenna has the measured antenna gain of around 5 dBic.

References

[1] S. Fu, S. Fang, Z. Wang, and X. Li, "Broadband circularly polarized slot antenna array fed by asymmetric CPW for L-band application," *IEEE Antennas Wireless Propag. Lett.*, vol. 8, pp. 1014–1016, 2009.

[2] J. Y. Sze, J. C. Wang, and C. C. Chang, "Axial-ratio bandwidth enhancement of asymmetric-CPW-fed circularly-polarised square slot antenna," *Electron. Lett.*, vol. 44, no. 18, pp. 1048–1049, Aug. 2008.

[3] T. N. Chang, "Circular polarized antenna for 2.3–2.7 GHz WiMAX band," *Microw. Opt. Technol. Lett.*, vol. 51, no. 12, pp. 2921–2923, Dec. 2009.

[4] S. H. Yeung, K. F. Man, and W. S. Chan, "A bandwidth improved circular polarized slot antenna using a slot composed of multiple circular sectors," *IEEE Trans. Antennas Propag.*, vol. 59, no. 8, pp. 3065–3070, Aug. 2011.

[5] J. Y. Sze, K. L. Wong, and C. C. Huang, "Coplanar waveguide-fed square slot antenna for broadband circularly polarized radiation," *IEEE Trans. Antennas Propag.*, vol. 51, no. 8, pp. 2141–2144, Aug. 2003.

[6] J. Y. Sze and C. C. Chang, "Circularly polarized square slot antenna with a pair of inverted-L grounded strips," *IEEE Antennas Wireless Propag. Lett.*, vol. 7, pp. 149–151, 2008.

[7] Q. X. Chu and S. Du, "A CPW-fed broadband circularly polarized square slot antenna," *Microw. Opt. Technol. Lett.*, vol. 52, no. 2, pp. 409–412, Feb. 2010.

[8] T. N. Chang, "Wideband circularly polarised antenna using two linked annular slots," *Electron. Lett.*, vol. 47, no. 13, pp. 737–739, Jun. 2011.

[9] J. Pourahmadazar and S. Mohammadi, "Compact circularly-polarised slot antenna for UWB applications," *Electron. Lett.*, vol. 47, no. 15, pp. 837–838, Jul. 2011.

[10] J. Y. Sze, C. G. Hsu, Z. W. Chen, and C. C. Chang, "Broadband CPW-fed circularly polarized square slot antenna with lightening-shaped feedline and inverted-L grounded strips," *IEEE Trans. Antennas Propag.*, vol. 58, no. 3, pp. 973–977, Mar. 2010.

[11] N. Felegari, J. Nourinia, C. Ghobadi, and J. Pourahmadazar, "Broadband CPW-fed circularly polarized square slot antenna with three inverted-L-shape grounded strips," *IEEE Antennas Wireless Propag. Lett.*, vol. 10, pp. 274–277, Apr. 2011.

[12] J. Pourahmadazar and V. Rafii, "Broadband circularly polarised slot antenna array for L and S-band applications," *Electron. Lett.*, vol. 48, no. 10, pp. 542–543, May 2012.

[13] J. Y. Jan and C. Y. Hsiang, "Wideband CPW-fed slot antenna for DCS, PCS, 3G and bluetooth bands," *IEE Electron. Lett.*, vol. 42, pp. 1377–1378, Nov. 2006.

A Topology-Based Miniaturization of Circularly Polarized Patch Antennas

Jungsuek Oh and Kamal Sarabandi

***Abstract*—A novel approach for the miniaturization of circularly polarized patch antennas is presented. This enables a size reduction of as high as 75%, compared to a conventional corner-truncated circularly polarized patch antenna. The proposed design procedure consists of a number of intermediate steps, each of which produces antenna miniaturization as well as the desired polarization and impedance matching properties. This is very challenging in miniaturizing circularly polarized probe-fed patch antennas. It is shown that two resonant frequencies can be tuned independently to produce a dual band antenna with two orthogonal polarizations. Finally, two circularly polarized miniaturized patch antennas with different miniaturization factors are fabricated, and their input impedances, radiation patterns and axial ratios are discussed.**

***Index Terms*—Anisotropic media, circularly polarized antennas, microstrip antennas.**

I. Introduction

Many modern satellite and terrestrial point-to-point communications systems use circularly polarized (CP) waves in order to maximize the polarization efficiency and thus improve the propagation link budget [3]. Although a CP antenna with a low profile, small size and light weight is highly desirable in many applications such as compact satellite or mobile platforms [4], most miniaturization techniques are developed for linearly polarized antennas [5]–[7]. This is mainly due to the fact that antennas with extremely small lateral dimensions are incapable of internally generating the required conditions for CP operations.

Many compact CP patch antennas have been proposed and investigated [8]–[10]. These efforts have relied mainly on intuitive techniques such as inserting several slots or slits in suitable locations on the patch itself. In such antenna designs, the splitting of two near-degenerate orthogonal modes with equal amplitudes and a 90° phase difference is achieved by slightly adjusting the embedded slots, such as a cross-slot in a patch or slits at the boundary of the patch. Theses inserted slots

Manuscript received September 20, 2011; revised October 25, 2012; accepted November 15, 2012. Date of publication December 04, 2012; date of current version February 27, 2013. This work was supported by the U.S. Army Research Laboratory under contract W911NF and prepared through collaborative participation in the Microelectronics Center of Micro Autonomous Systems and Technology (MAST) Collaborative Technology Alliance (CTA).

The authors are with the Radiation Laboratory, Department of Electrical Engineering and Computer Science, The University of Michigan at Ann Arbor, Ann Arbor, MI 48109-2122 USA (e-mail: jungsuek@umich.edu; saraband@eecs.umich.edu).

Digital Object Identifier 10.1109/TAP.2012.2231915

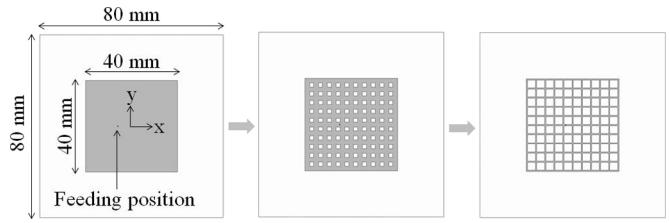

Fig. 1. Conversion of a $\lambda_g/2$ microstrip antenna to an array of thin wires.

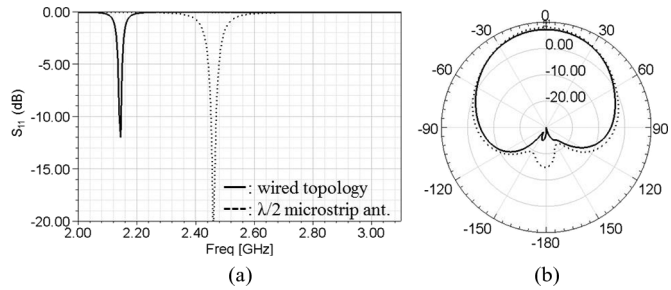

Fig. 2. Simulated (a) S_{11} and (b) radiation pattern on xz-plane of a wire mesh patch antenna and a conventional $\lambda_g/2$ microstrip antenna with the same sizes and substrate.

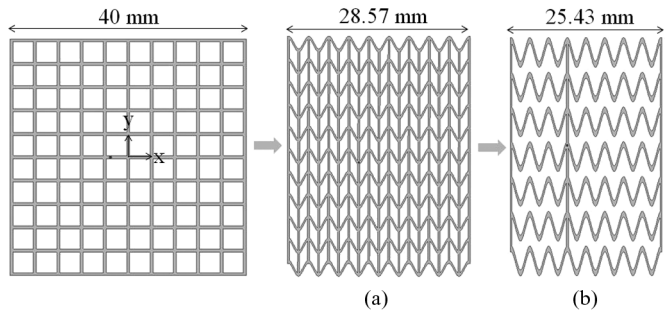

Fig. 3. (a) Shrunk wires and (b) sinusoidal wires with the elimination of wires in parallel with y-axis.

and slits force redirection of the excited fundamental-mode surface current and also cause the resonant frequency to be shifted down to some extent. However, this approach has yielded somewhat limited miniaturization due to lack of ability to simultaneously control the surface current paths as well as create the required 90° phase difference. It is shown that these methods can provide size reductions of as low as 50%. Although a size reduction of about 70% is also reported, the area covered by the feed structure makes the overall size bigger. This is due to the fact that such antennas with higher size reductions are not compatible with the direct probe-fed method since no 50 Ω feed positions exist inside the microstrip patch due to the large cross-slot cut inside the patch [1], [2].

This communication presents a new miniaturized circularly polarized (CP) probe-fed patch antenna. Section II presents a miniaturized linearly polarized patch antenna formed by an anisotropic conductor. Section III introduces a topology modification for generating two orthogonal modes, and Section IV shows antenna topology designs for achieving circular polarization. Section V describes a topology optimization process for size reduction. Details in each design step and measurement results are discussed, and a size reduction of as high as 75% is demonstrated, as compared to the conventional corner-truncated CP square microstrip antenna.

II. Miniaturization of Linearly Polarized Patch Antennas Using Meandered Metallic Traces

A. Wire-Mesh Microstrip Patch Antenna

The proposed design approach for miniaturizing circularly polarized patch antennas starts from the miniaturization of a linearly polarized microstrip antenna using an anisotropic conductor. The anisotropic conductor is formed by removing parallel thin metal strips from the conventional microstrip antenna. The concept of the modified topology begins by considering electric current distribution on an ordinary rectangular microstrip antenna at its fundamental mode. In this case, the electric current is primarily parallel to one edge with a sinusoidal intensity variation attaining a null value at the edge. On the other hand, the electric field under the patch has maxima where the electric current is zero, forming two parallel fictitious magnetic currents responsible for the radiation of the patch antenna. Considering an ordinary $\lambda_g/2$ microstrip antenna with linear polarization along the x-axis (where $\lambda_g = \lambda_0/\sqrt{\epsilon_r}$, $\lambda_0 = \text{free} - \text{space wavelength}$ and $\epsilon_r = 2.2$), the progression of topology modification is shown in Fig. 1. The uniform metallic patch is replaced with a mesh which can be thinned out without performance loss so long as the mesh dimensions are roughly smaller than $\lambda_g/15$. Basically, the radiation pattern is not changed, but the resonant frequency is reduced slightly. This is due to the fact that thin wires have some additional inductance per unit length. To demonstrate this, the metallic patch and the wire mesh version are simulated assuming perfect electric conductor (PEC) (ignoring ohmic loss) using Ansoft HFSS 12.1.

Fig. 2 shows the simulated return loss (S_{11}) and E-plane radiation patterns (xz-plane) of the wire mesh and the original $\lambda_g/2$ microstrip antenna. The gains of both antennas are about 7 dBi. The lateral dimension of the $\lambda_g/2$ microstrip antenna is 40 mm, and the thickness and dielectric constant of the substrate are 3.175 mm and 2.2, respectively. The size of the ground plane is 80 mm × 80 mm. The wire mesh antenna is designed with the same substrate and physical dimensions. As explained above, the resonant frequency of the wire mesh antenna is shifted down by about 10%.

B. Accordion Topology for Size Reduction

Straight wires in Fig. 1 are meandered to fit a longer path length in a given dimension, leading to the miniaturization of the linear dimension along the x-axis, as shown in Fig. 3(a). From this design step, the conductivity of copper is used in all metallic traces to consider ohmic loss. In order to reduce ohmic loss, the sharp edges of the meandered wires are made to be smoother, giving it a sinusoidal shape, as shown in Fig. 3(b). In addition, all metallic traces in parallel with the y-axis are eliminated, creating an anisotropic conductor, except for two wires at both ends and a wire connected with a feed probe. The end conductor strips are needed to facilitate uniform vertical electric fields between the conductors and the ground plane, which produces in-phase equivalent magnetic currents.

The topology shown in Fig. 3(b) still works as a linearly x-polarized antenna. As depicted in Fig. 4(b), the gain of this antenna is 5.5 dBi. The linear dimensions in both the x and y directions of the area covered by antenna pattern are 25.43 mm ($= 0.29\lambda_g$) and 40 mm ($= 0.46\lambda_g$), respectively. This renders a size reduction of 40%, compared to the conventional microstrip antenna.

III. Excitation of Two Near-Degenerate Orthogonal Modes

Starting with the accordion-shape patch antenna with linear polarization, modifications are sought to generate a simultaneous orthogonal polarization. Examining the topology shown in Fig. 3(b), it is obvious that y-directed electric surface currents can only be excited on the three y-directed wires. If a new resonance can be created by the currents, then y-polarized radiation can also be generated. It is found that two wires

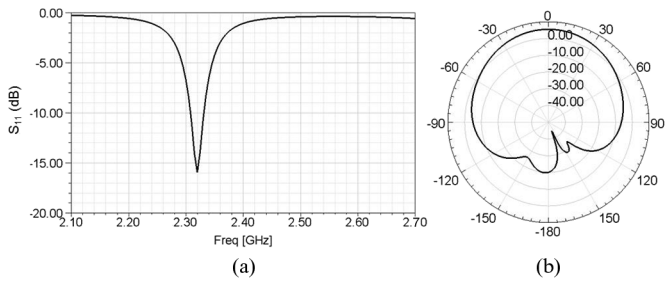

Fig. 4. Simulated (a) S_{11} and (b) radiation pattern on xz-plane of the wired antenna depicted in Fig. 3(b).

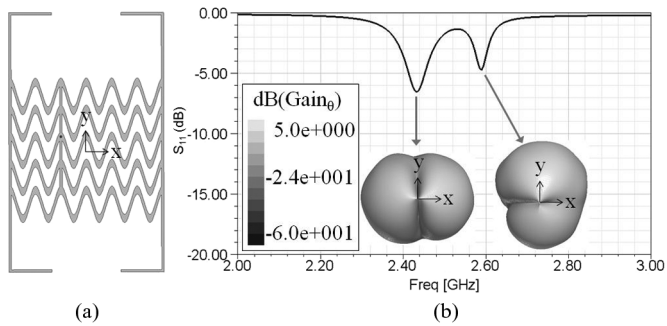

Fig. 5. (a) Topology of a dual polarized antenna and (b) simulated S_{11} and θ-polarized 3D radiation patterns at two resonant frequencies.

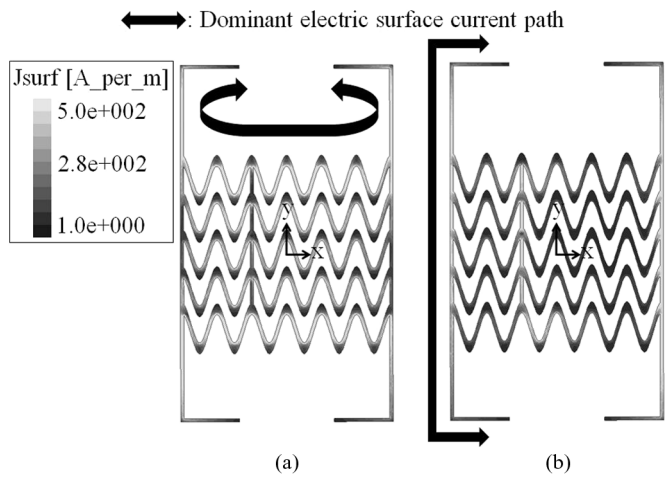

Fig. 6. Electric surface current distributions at the resonant frequencies where the antenna radiates (a) x- and (b) y-polarized fields.

at both ends can act like two y-directed $\lambda_g/2$ dipole antennas. Appropriately extending and then bending two end wires, an additional resonant frequency related to y-polarized radiation can be created. Fig. 5(a) shows the modified topology and Fig. 5(b) shows simulated S_{11} and θ-polarized 3D radiation patterns at two resonant frequencies. At the first resonant frequency, where x-polarized radiation is dominant, a radiation null exists on the y-axis, and at the second resonant frequency, the radiation null exists on the x-axis.

Fig. 6 shows electric surface current distributions at two resonant frequencies of the topology shown in Fig. 5(a). As expected, while the surface current on the x-directed meandered wires is dominant at the first resonant frequency, the surface current on the y-directed two wires at both ends is dominant at the second resonant frequency.

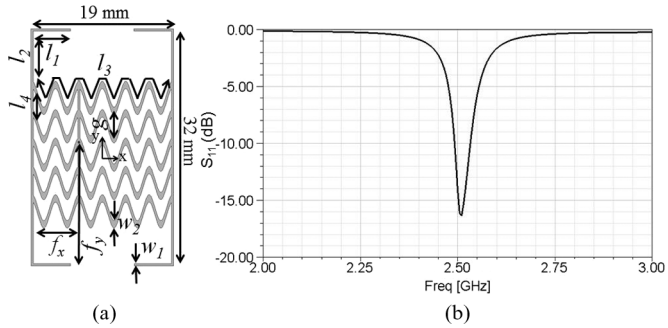

Fig. 7. (a) Topology, design parameters and (b) simulated S_{11} of the proposed CP antenna exhibiting 59% size reduction as compared to the conventional corner-truncated square microstrip antenna.

IV. Design of Miniaturized CP Patch Antennas

In order to design a CP antenna using the topology shown in the previous section, the two resonant frequencies corresponding to two orthogonal modes must be at the same frequency, and the two orthogonal linearly polarized components of the radiated fields must have equal amplitudes and a 90° phase difference. This requirement makes the miniaturization of CP antennas very difficult because the behaviors of the antenna at the two resonant frequencies must be controlled independently.

Considering the dominant electric surface current paths shown in Fig. 6, geometrical features must be extracted to independently tune the two resonant frequencies. Fig. 7(a) shows these tuning geometrical features of the structure. While l_1 and l_2 affect both the resonant frequencies, l_3 and l_4 only affect the electrical length related to the x-pol and y-pol, respectively. Varying these parameters simultaneously in such routines, the two split resonant frequencies can be merged into a single frequency with an acceptable return loss value as shown in Fig. 7(b). To achieve impedance matching with a 50 Ω feed probe, parameters ($= f_x$ and f_y) related to a feeding position are appropriately optimized as well. The linear dimensions in both the x and y directions of the area covered by the antenna topology are 19 mm and 32 mm, respectively. This produces a size reduction of 59%, compared to a corner-truncated CP square microstrip antenna on the same substrate. In other words, the area of the proposed antenna is just 41% of that of a conventional CP square microstrip antenna. The values of other design parameters are given by $l_1 = 5$ mm, $l_2 = 6.86$ mm, $l_3 = 46.3$ mm, $l_4 = g = 2.83$ mm, $f_x = 6.13$ mm, $f_y = 16.1$ mm, $w_1 = 0.3$ mm and $w_2 = 1$ mm. For the sinusoidal meandering, a function of the form $\mathrm{y} = 1.7\cos(2\times)$ is used where the argument is in radian and the value of the x dimension in millimeters is inserted.

It is interesting to note that if the positions of two resonant frequencies are moved slightly with respect to each other, both right-handed (RH) and left-handed (LH) CP can be obtained. When the resonant frequency of the x-pol is slightly lower than that of the y-pol, the antenna radiates with RHCP. Contrary to this, when the resonant frequency of the y-pol is slightly lower than that of the x-pol, the antenna radiates with LHCP. Fig. 8 shows a simulated axial ratio of the antenna shown in Fig. 7(a). The 3 dB axial ratio bandwidth is about 0.8%. Good RHCP radiation is observed in Fig. 9. The antenna gain (RHCP) in the broadside direction is 5 dBi which is 2 dB lower than the conventional corner-truncated square microstrip antenna due to size reduction.

V. Additional Size Reduction by Simplifying Antenna Geometry

In this section, it is shown that additional size reduction can be achieved by modifying l_1, l_2, l_3, l_4 and the number of sinusoidal traces used in Fig. 7(a). The same principle described in the previous

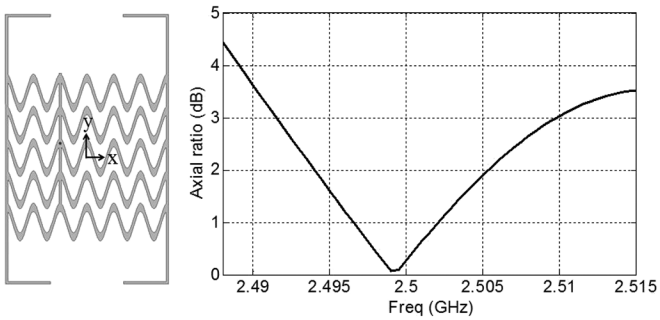

Fig. 8. Simulated axial ratio in the broadside direction for the antenna shown in Fig. 7(a).

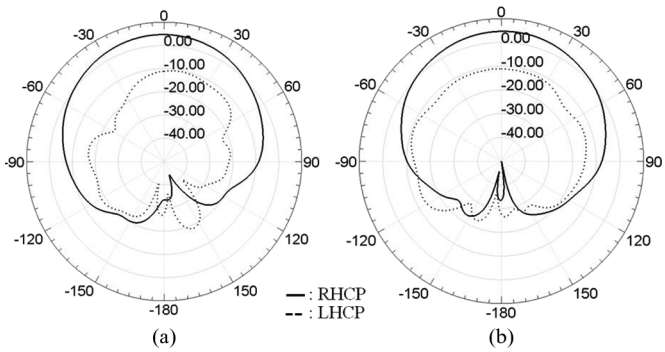

Fig. 9. Simulated radiation patterns in two orthogonal planes of (a) xz and (b) yz-planes for the antenna shown in Fig. 7(a).

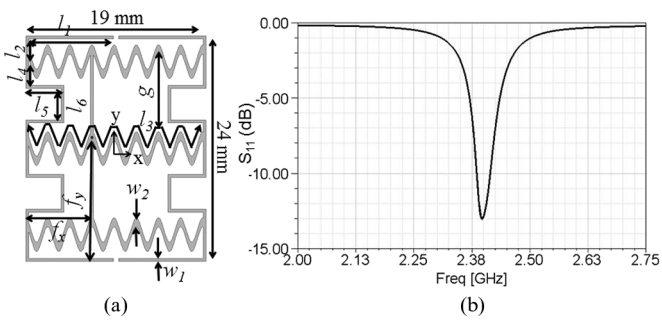

Fig. 10. (a) Topology, design parameters and (b) simulated S_{11} of the proposed CP antenna exhibiting 72% size reduction as compared to the conventional corner-truncated square microstrip antenna.

section is applied. Extending l_1 and l_2 leads to lowering both resonant frequencies. While l_3 works only for the extension of the x-directed surface current path, l_4 does for the y-directed surface current path. It is found that the number of sinusoidal traces can be reduced from 5 in Fig. 7(a) to 3 in Fig. 10(a), without affecting the dominant electric surface current paths. The space generated by eliminating 2 sinusoidal traces enables further size reduction since l_4 in Fig. 7(a) can be extended to $2^*(l_4 + l_5) + l_6$ in Fig. 10(a). As mentioned earlier, since l_4 in Fig. 7(a) is related to the y-polarized electrical length, the linear dimension of this antenna along the y-axis can be reduced from 32 mm in Fig. 7(a) to 24 mm in Fig. 10(a) while maintaining the antenna dimension along the x-axis as 19 mm.

Fig. 10 shows the topology and simulated S_{11} of the proposed CP antenna exhibiting 72% size reduction compared to the conventional corner-truncated CP square microstrip antenna. The antenna is designed to radiate with LHCP. The values of the design parameters are given by $l_1 = 9$ mm, $l_2 = 1.15$ mm, $l_3 = 46.37$ mm, $l_4 = 2.8$ mm,

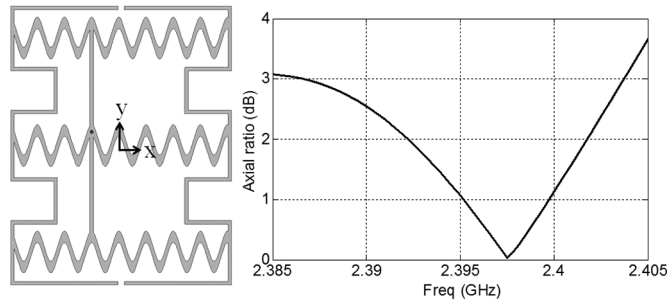

Fig. 11. Simulated axial ratio in the broadside direction for the antenna shown in Fig. 10(a).

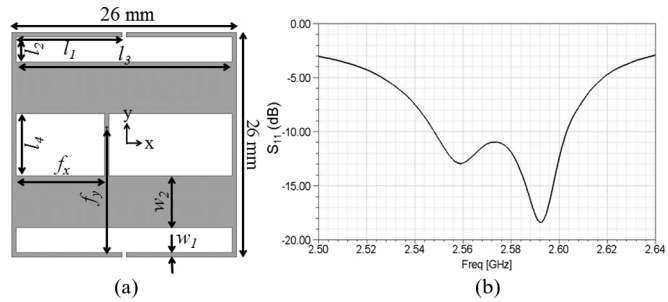

Fig. 12. (a) Topology, design parameters and (b) measured S_{11} of the proposed CP antenna exhibiting 53% size reduction as compared to the conventional corner-truncated square microstrip antenna.

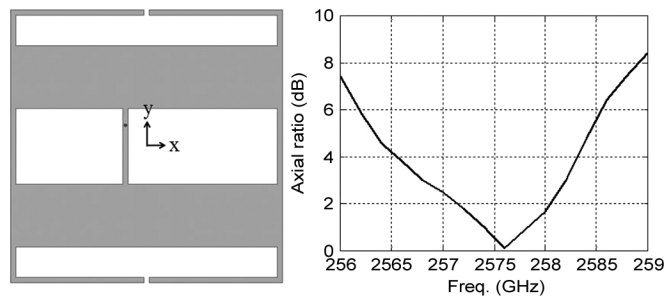

Fig. 13. Measured axial ratio in the broadside direction for the antenna shown in Fig. 12(a).

$l_5 = 3.75$ mm, $l_6 = 3.4$ mm, $g = 8.15$ mm, $f_x = 6.57$ mm, $f_y = 12.9$ mm, $w_1 = 0.3$ mm and $w_2 = 1$ mm. For sinusoidal meandering, the function of $y = -1.3\sin(8/3^* \times)$ is used. Fig. 11 shows the simulated axial ratio of the antenna in Fig. 10(a). The 3 dB axial ratio bandwidth of 0.6% is computed.

Lastly, further reducing the number of sinusoidal traces from 3 in Fig. 10(a) to 2 achieves more simplified antenna geometry. Fig. 12(a) shows that the topology and design parameters of the simplified antenna geometry exhibit a size reduction of 53% compared to the conventional corner-truncated square microstrip antenna. The effects of the design parameters shown in Fig. 12(a) are the same as explained in the previous sections. While l_3 and w_2 affect the resonant frequency of the x-pol, l_4 does so for the y-pol. It should be noted that while those design parameters independently affect the resonant frequencies of the two orthogonal modes, they constrain each other in some ways. For example, in order to increase l_4, w_2 should decrease when other design parameters and physical dimension of the antenna are fixed. Considering this limitation and the characteristics of the design parameters, an antenna with LHCP and a size reduction of 53% is designed and fabricated. The values of the design parameters are given

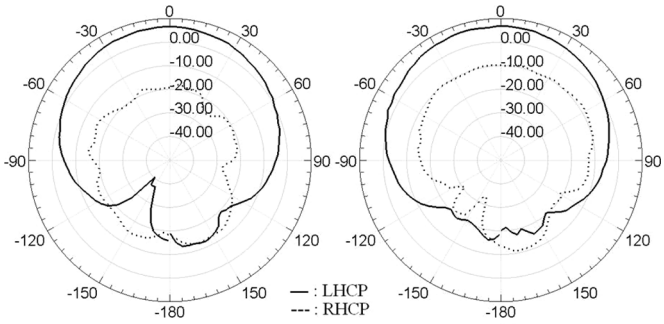

Fig. 14. Measured radiation patterns in two orthogonal planes of (a) xz and (b) yz-planes for the antenna shown in Fig. 12(a).

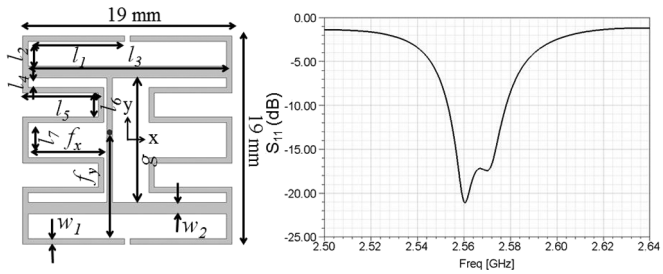

Fig. 15. (a) Topology, design parameters and (b) measured S_{11} of the proposed CP antenna exhibiting 75% size reduction as compared to the conventional corner-truncated square microstrip antenna.

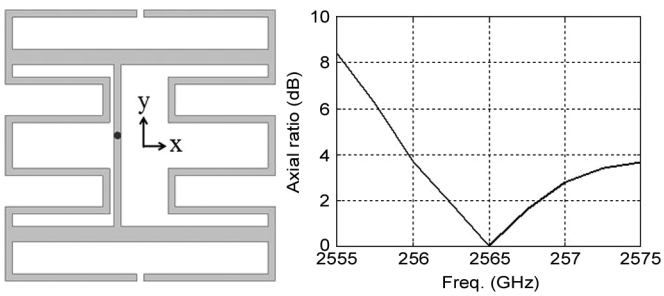

Fig. 16. Measured axial ratio in the broadside direction for the antenna shown in Fig. 15(a).

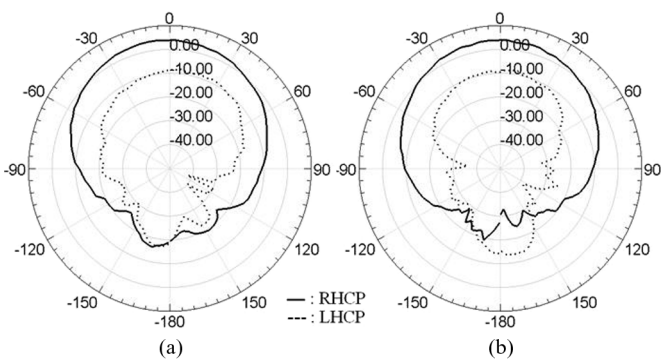

Fig. 17. Measured radiation patterns in two orthogonal planes of (a) xz and (b) yz-planes for the antenna shown in Fig. 15(a).

by $l_1 = 12.25$ mm, $l_2 = 2.9$ mm, $l_3 = 25$ mm, $l_4 = 7.2$ mm, $f_x = 10.5$ mm, $f_y = 14.5$ mm, $w_1 = 0.5$ mmand $w_2 = 6$ mm. The measured S_{11} in Fig. 12(b) indicates an input impedance matching of better than 10 dB at the two resonant frequencies corresponding to the two orthogonal polarizations and the center frequency of 2.576 GHz. This design also demonstrates that by separating the two resonant frequencies, a wider impedance bandwidth can be achieved. As shown in Fig. 13, the 3 dB axial ratio bandwidth of 0.7% is measured. The measured radiation patterns in two orthogonal planes of the xz and yz-planes are presented in Fig. 14. As expected, this figure shows a smooth LHCP pattern with excellent suppression of RHCP radiation.

Substituting l_4 in Fig. 12(a) by $2^*l_4 + 4^*l_5 + 2^*l_6 + l_7$ in Fig. 15(a) and optimizing the other design parameters, further size reduction can be achieved. An antenna with RHCP and a size reduction of 75% is designed and fabricated. The values of the design parameters are given by $l_1 = 8.75$ mm, $l_2 = 2.25$ mm, $l_3 = 18$ mm, $l_4 = 0.85$ mm, $l_5 = 6.85$ mm, $l_6 = 2.2$ mm, $l_7 = 3.2$ mm, $f_x = 7.4$ mm, $f_y = 9.7$ mm, $w_1 = 0.5$ mm and $w_2 = 1.1$ mm. The measured S_{11} is shown in Fig. 15(b) with excellent impedance matching at two slightly different resonant frequencies. The center frequency of the antenna is 2.565 GHz and its 10 dB return loss bandwidth is 25 MHz. As is the case with the other presented antennas, impedance matching with a 50 Ω feed probe is obtained by changing f_x and f_y. Fig. 16 and 17 show the measured axial ratio and radiation patterns of the antenna, respectively.

VI. Conclusion

A novel approach for the miniaturization of circularly polarized patch antennas is presented. The initial approach is based on shrinking the resonant dimension by transforming the patch antenna into a wire-mesh and then squeezing it in accordion fashion. The topology of the meandered wire mesh antenna is simplified while maintaining the original linear polarization property. By tailoring the paths of the dominant electric surface currents on the simplified antenna topology, two near-degenerate orthogonal modes are created. This enables the design of miniaturized CP antenna configurations. The proposed design method is validated by measurement results. It is shown that a size reduction of as high as 75% can be achieved compared to the conventional corner-truncated square microstrip antenna.

References

[1] K. L. Wong and Y. F. Lin, "Circularly-polarised microstrip antenna with tuning stub," *Electron. Lett.*, vol. 34, no. 9, pp. 831–832, Apr. 30, 1998.

[2] K. L. Wong and M. H. Chen, "Small slot-coupled circularly-polarised microstrip antenna with modified cross-slot and bent tuning-stub," *Electron. Lett.*, vol. 34, no. 16, pp. 1542–1543, Aug. 6, 1998.

[3] B. Y. Toh, R. Cahill, and V. F. Fusco, "Understanding and measuring circular polarization," *IEEE Trans. Education*, vol. 46, p. 313, Aug. 2003.

[4] D. M. Pozar and S. M. Duffy, "A dual-band circularly polarized aperture-coupled stacked microstrip antenna for global positioning satellite," *IEEE Trans. Antennas Propag.*, vol. 45, pp. 1618–1625, Nov. 1997.

[5] N. Behdad and K. Sarabandi, "Bandwidth enhancement and further size reduction of a class of miniaturized slot antennas," *IEEE Trans. Antennas Propag.*, vol. 52, no. 8, pp. 1928–1935, Aug. 2004.

[6] W. Hong and K. Sarabandi, "Low-profile, multi-element, miniaturized monopole antenna," *IEEE Trans. Antennas Propag.*, vol. 57, pp. 72–80, Jan. 2009.

[7] J. Oh and K. Sarabandi, "Low profile, miniaturized, inductively coupled capacitively loaded monopole antenna," *IEEE Trans. Antennas Propag.*, vol. 60, pp. 1206–1213, Mar. 2012.

[8] H. Iwasaki, "A circularly polarized small-size microstrip antenna with a cross slot," *IEEE Trans. Antennas Propag.*, vol. 44, pp. 1399–1401, Oct. 1996.

[9] W. S. Chen, C. K. Wu, and K. L. Wong, "Compact circularly polarized microstrip antenna with bent slots," *Electron. Lett.*, vol. 34, pp. 1278–1279, Jun. 25, 1998.

[10] W. S. Chen, C. K. Wu, and K. L. Wong, "Novel compact circularly polarized square microstrip antenna," *IEEE Trans. Antennas Propag.*, vol. 49, pp. 340–342, Mar. 2001.